

Analysis and Performance Validation of CRONE Controllers for Speed Control of a DC Motor

V. Velmurugan ^{a,1,*}, M. Venkatesan ^{b,2}, N. N. Praboo ^{c,3}

^a Department of EEE, Arunai Engineering College, Tiruvannamalai, Tamilnadu, India

^b Department of ECE, Dhanalakshmi Srinivasan College of Engineering, Coimbatore, Tamilnadu, India

^c Department of EIE, Annamalai University, Annamalaiagar, Tamilnadu, India

¹ velnathan@gmail.com; ² venkatesangct@gmail.com; ³ praboonn@gmail.com

* Corresponding Author

ARTICLE INFO

ABSTRACT

Article history

Received March 07, 2024

Revised April 21, 2024

Accepted May 06, 2024

Keywords

First Generation CRONE;

Second Generation CRONE;

Control System Design

Toolbox;

DC Motor;

Relay PI Controller

In recent decades controllers play a major role for an efficient control and reliable operation of an industrial process. Hence in this paper, a special kind of Commande Robuste d'Ordre Non Entier (CRONE) controller is designed for controlling the speed of DC Motor (DCM). The proper design procedure of two generations CRONE control strategies named as First-Generation CRONE (FGC) and Second-Generation CRONE (SGC) controllers are implemented through the transfer function of armature-controlled DCM. Simulations are performed on MATLAB software in order to investigate the servo responses of two designed CRONE controllers, besides the results are presented in terms of settling time(t_s), rise time(t_r), Integral Square Error (ISE) and Integral Absolute Error (IAE). In addition, the relay PI controller is designed and the simulation results are presented for comparison purpose. It is evident from the comparing results that the SGC controller is superior for effective process control.

This is an open-access article under the [CC-BY-SA](https://creativecommons.org/licenses/by-sa/4.0/) license.



1. Introduction

In many decades, the controllers are playing a major role for an efficient control and reliable operation of an industrial process, especially the integer controller is dominating in time domain approaches for the controlling the electrical systems. Several researchers have been concentrating the design of the non-integer order controller [1], [2] in the frequency domain approaches. The noninteger order controller has shown its superiority over the controller that developed naturally in the environment in recent years and has played a significant role in the industry, particularly in the automation sector. Alian Oustaloup first made the non integer controller public in 1991 [3], [4].

He introduced the controller community to the CRONE controller, a specialized non-integer type of controller. It stands for "Commande Robuste d'Ordre Non Entiere," a robust controller based on a frequency domain approach. The FGC [5] controller maintains the plant's robustness and offers a steady phase margin around the gain cross over frequency (ω_{gc}) when the plant parameter changes. However, the SGC [6]-[12] controller guarantees a consistent damping ratio and resonance ratio by directly removing phase variation during reparameterization. The CRONE controller for heat exchangers has been proposed to maintain and manage parameter fluctuation in the specified

process. The CRONE controller was tweaked using meta-heuristic methods, such as the Whale Optimization Algorithm (WOA) and Grey Wolf Optimization (GWO) algorithms [13].

A time delayed system using CRONE controller has been designed to obtain a robust stability of the system by interval analysis method. The controller has designed for SISO system, which is the limitation of this paper [14]. The mathematical expression for the Fractional- Order controller (FOC) has been derived in continuous and discrete form to design a controller. The designed FOC implemented to control the speed of permanent magnet DCM and the results have examined in terms of stability. A detailed study of introduction to FC and their background control theory has been presented [15], [16]. A fractional order Proportional Integral Controller (FO-PIC) has been designed and implemented for a liquid level system and the performances have examined in terms of ISE and IAE [17].

The FOC ($PI^\lambda D^\mu$) controller has been developed to fulfill five different design specifications for the closed-loop system, taking their advantages if the fractional order of λ and μ towards to obtain robust performance [18]. The FOC has been implemented utilizing an operational transconductance amplifier and the controller allows finding the control characteristics of the DCM [19]. The industry commonly use a novel technique for effective speed regulation of micro motors, known as Fractional-Order Proportional Integral Derivative (FOPID) controller, which is based on the Gazelle Optimization Algorithm (GOA). Finally, the performance of the GOA controller and other heuristic advanced controllers were compared [20]. The nonlinearities of DCM have been discussed and identified the robustness of various controllers by comparative result of the four different model [21]-[23]. Multivariable robust controller has been proposed to regulate an angular speed of DCM and active current sharing in DC/DC buck converter. The converter connected serially to the armature of DCM, besides the controller rejects internal and external disturbances [24].

The new discrete type of generalized proportional-integral observer (GPIO) has been used to measure the uncertainties and output speed prediction of DC-DC buck converter driven DCM. The uncertainties are regulated by using discrete-time model predictive control algorithm [25]. It has been reported to control speed of brushed DCM with small armature is difficult using PWM signal owing development of heat during the operation. However, the speed of the system can be regulated by back emf and the performance verified in simulation and measurement. Although, the author suggested that PI controller required to control speed of small armature using PWM [26]-[29]. A controller has been designed to control the speed of permanent magnet DCM and the performances compared with solutions obtained by prototype experiment model [30], [31].

The vehicle longitudinal motion control was obtained by Cruise Control system with need of CRONE controller and comparison made with classical PI and H- α controller solutions [32]. A novel fractional-order robust lead-lag controller was designed for an unstable system and its performance compared with H $_{\alpha}$ controller through simulation results [33]. The performance analysis for the discrete fractional order PID controller in the presence of nonlinearities and output backlash has been discussed [34], [35]. The predictive control algorithm has been proposed for controlling the speed of a DC motor using a DC-DC converter and exhibiting the performance of its utilization in electrical vehicles [36]. The speed control of DCM has been achieved using a classical PID controller and has been tested at various loads to obtain performance characteristics [37]-[39]. The FO-PID controller has been designed to control the speed of armature-controlled DCM and liquid level control. The comparative solutions have presented [40]-[42].

A Fuzzy PID controller has been developed to control the BLDC motor during the load removal condition of dynamic characteristic and the solutions compared with PID controller performance. Also, PI and Fuzzy controller has been utilized for multilevel inverter [43]-[47]. The FO-PID controller has been designed using constant phase technique. The parameters of the controllers have identified based on particles swarm optimization technique and implemented using floating point digital signal processor for controlling the speed of separately excited DCM [48]. An artificial intelligence has been presented to estimate the power consumption of brushless DC motor based on finite element analysis [49]. A FO-PID controller has now been designed to control torque

and speed of brushless DCM. Firefly algorithm has employed in order to tune the controller for obtaining the effective control torque and speed. The performance of proposed FO-PID controller has compared with GA based FO-PID controller through solutions [50].

Based on the above findings, it is decided to propose a special kind of controllers in this work. Two generations of CRONE control strategies named as FGC and SGC are designed to control the speed of DC motor. In addition, relay PI controller is designed in order to make comparative analysis. The simulation is carried out using in MATLAB/Simulink environment and expedited by CRONE CSD (Control System Design) toolbox [51], [52].

The research work is explained as follows: In Section 2 described process description and determination of DCM transfer function model using analytical approach. The control strategy for the two generation of CRONE controller and relay PI controller is considered in Section 3. Section 4 discusses design methodology of CRONE controller. The simulation results of two generation of CRONE controller and relay PI controller deliberated in Section 5. Finally, the declaring results are given in Section 6.

2. Process Description

Fig. 1 gives information on speed control of DCM [19], which includes separately excited DCM, DC chopper unit, optocoupler sensor, personal computer and V-MAT card. The speed is controlled by armature voltage applied through chopper element since its conversion of Pulse Width Modulated (PWM) signal from personal computer. The V-MAT card interface DCM with personal computer. Optocoupler is used to sense the motor speed and converts in the form of pulses, then which is feed to computer through chopper circuit along with V-MAT card. Further the signal is compared with predefined signal to generate error signal. The error signal is applied to controller and generates controller output and it is applied to DCM [21] with help of chopper circuit in form of voltage. The DCM speed is controlled and monitored by the computer with need of MATLAB Simulink environment. Table 1 shows the real-time parameters of a DCM [22].

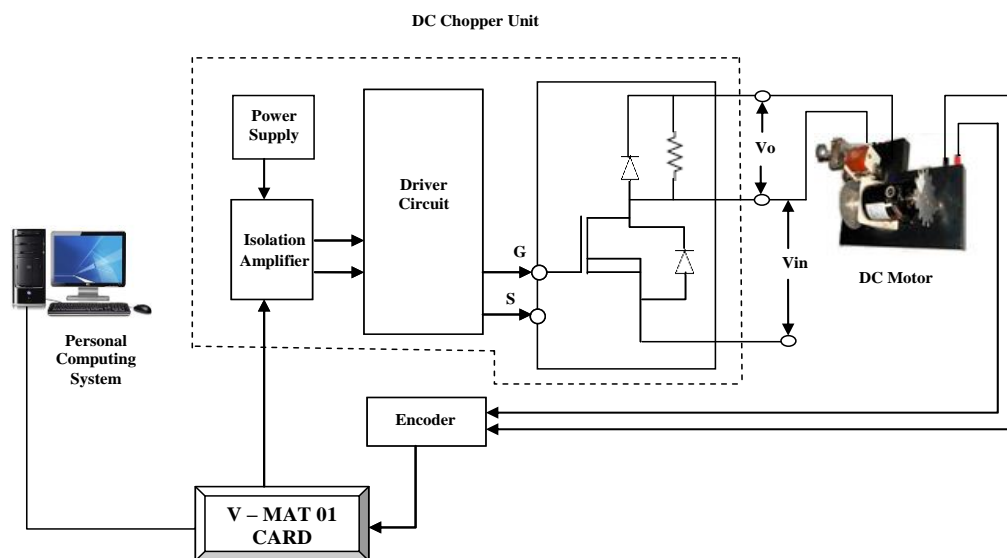


Fig. 1. Block diagram of speed control of DCM

Table 1. The Experimental setup parameters of DCM

Moment of Inertia of the rotor	$J = 0.04 \text{ kgm}^2$
Maximum Speed of the motor	1600 rpm
Damping (friction) of the mechanical system	$b = 0.021 \text{ Nms}$
$K_b = K_T = K$	$K = 0.1341$
Electric Resistance	$R = 7 \Omega$
Electric Inductance	$L = 4.6 \text{ mH}$

2.1. Mathematical Modelling of DCM Speed Control System

In this research work, separately excited DCM is considered to control the speed by varying voltage applied to the armature. The armature voltage is obtained by converting the PWM signal received from computer. The mathematical model of armature voltage controlled DCM is developed by considering equivalent circuit of DCM [23] as shown in Fig. 2.

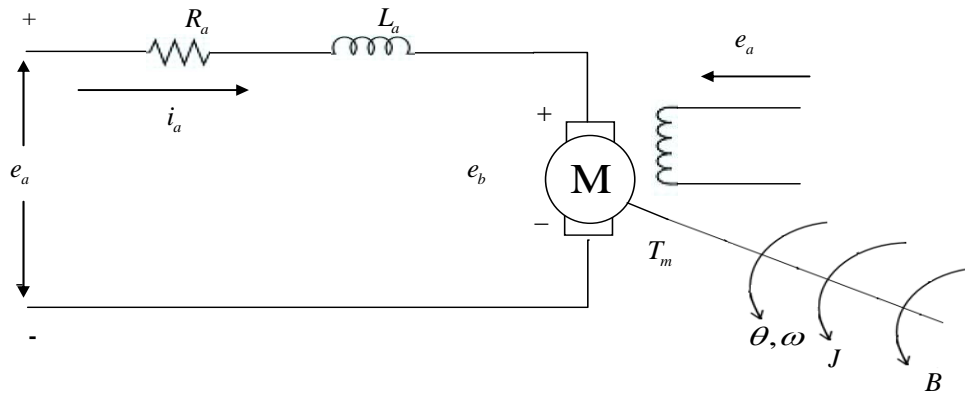


Fig. 2. Control circuit of the DC motor (armature voltage control)

It is known that the back emf is directly proportional to speed of the DCM as follows,

$$e_b(s) = k_b \frac{d\theta}{dt} = k_b \omega(t) \tag{1}$$

By applying KCL law,

$$e_a(t) = R_a i_a(t) + L_a \frac{di_a(t)}{dt} + e_b(t) \tag{2}$$

and making use of Newton law, the torque is

$$T_m = J \frac{d^2\theta(t)}{dt} + B \frac{d\theta}{dt} = K_T i_a(t) \tag{3}$$

Applying Laplace transform on both sides of the above equations we get as,

$$E_b(s) = K_b \omega(s) \tag{4}$$

$$E_b(s) = (R_a + L_a s) I_a(s) + E_b(s) \tag{5}$$

$$T_m(s) = Js^2 \omega(s) + Bs \omega(s) = K_T i_a(s) \tag{6}$$

Fig. 3 shows the block diagram for the DCM speed control system.

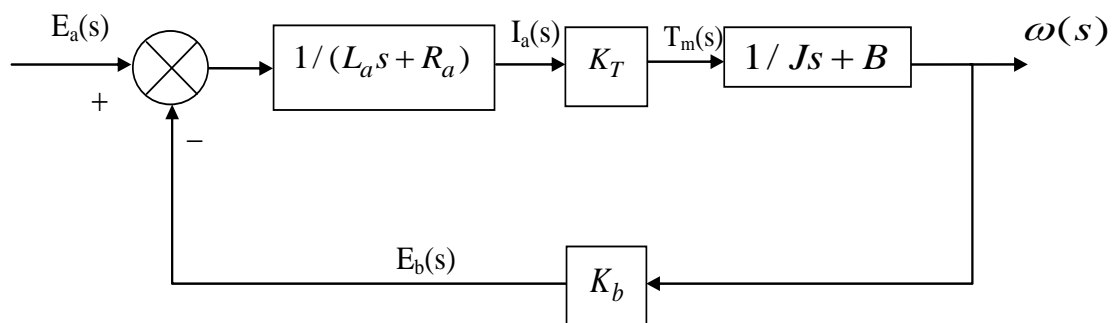


Fig. 3. Block diagram of armature voltage control of DC motor

The transfer function of speed control of DCM with applied input armature voltage is given as,

$$G(s) = \frac{\omega(s)}{E_a(s)} = \frac{K_T}{(L_a s + R_a)(J s + B) + K_b K_T} \quad (7)$$

2.2. Final Transfer Function Model of the Speed Control DCM System

The transfer function is determined by substitution of obtained practical value given in the Table 1 The system transfer function model is,

$$G(s) = \frac{\omega(s)}{E_a(s)} = \frac{1.01}{0.001025s^2 + 1.367s + 1} \quad (8)$$

3. CRONE Methodology

A MATLAB and Simulink toolbox devoted to fractional (or noninteger) derivative applications in science and engineering is called CRONE (Commande Robuste d'Ordre Non Entier), and it was progressively created by the CRONE research group during the 1990s. The toolbox is designed for both researchers and the industrial community, who are increasingly interested in fractional systems and willing to engage in application development. It is a frequency domain approach and is based on the common unity – feedback configuration. Three methods are available named as FGC, SGC and third generation CRONE (TGC) controllers.

3.1. FGC Controller

Fig. 4 demonstrates the block diagram of FGC [5] controller, which is based on the constant phase controller within a frequency range ω_A and ω_B around open loop gain cross over frequency (ω_{cg}).

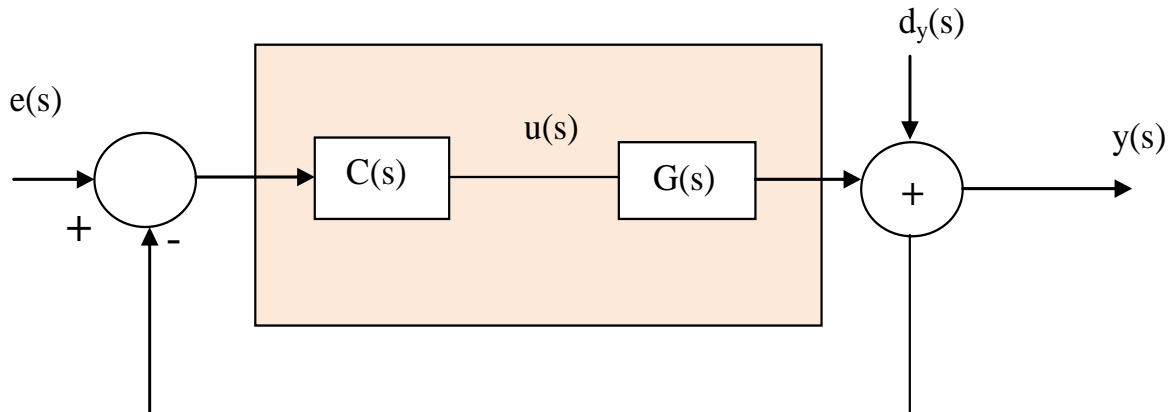


Fig. 4. Block diagram of FGC controller

The transfer function of ideal fractional order FGC controller is as follows,

$$C(s) = C_0 s^n, \text{ with } n \text{ and } C_0 \in \mathbb{R} \quad (9)$$

It is noticed from Fig. 5, FGC controller confirm the constant phase ($n\pi/2$) around open loop gain cross over frequency.

Fig. 5 represents bode plot of FGC [5] controller. The constant phase controller ($C_F(s)$) does not alter the phase margin when the plant gain or plant corner frequency changes. Since the gain crossover frequency ω_{cg} changes within a certain range, the frequency range $[\omega_A, \omega_B]$ must also equal that range. In the event that the plant exhibits order p behaviour asymptotically, the phase margin M_p is equivalent to $(n+p)/2$. Another way to define the FGC controller $C_F(s)$ is by a band-limited transfer function that uses the corner frequencies ω_l and ω_h as.

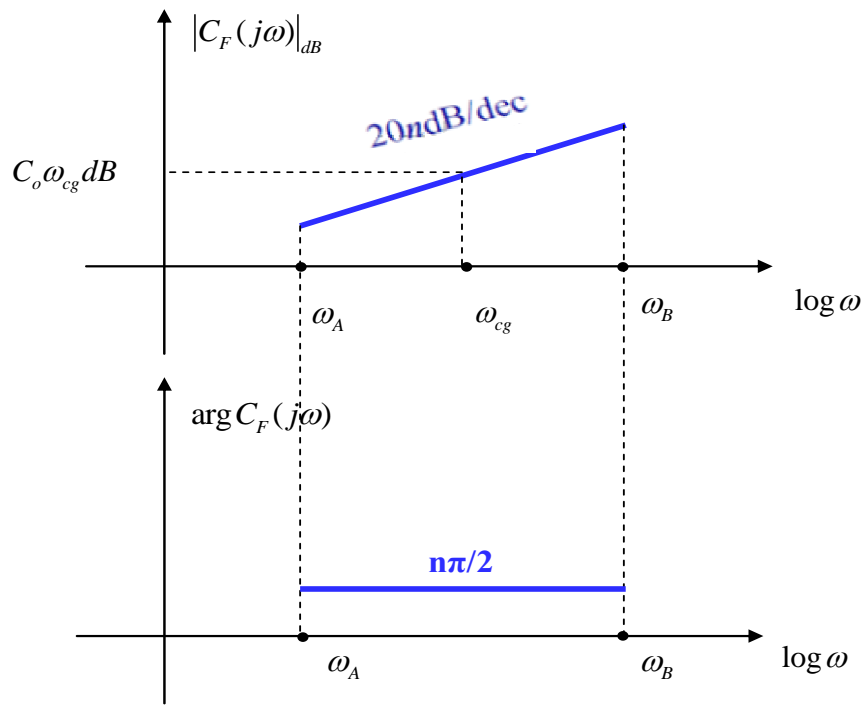


Fig. 5. Bode plot of FGC controller

$$C_F(s) = C_0 \left(\frac{1+s/\omega_l}{1+s/\omega_h} \right)^n, \omega_l < \omega_A \text{ and } \omega_h > \omega_B. \tag{10}$$

The above-mentioned transfer function does not exist in an implementable form and must be changed into an implementable form using the recursive distribution technique. The introduction of the real negative poles and zeros for the method of recursive distribution converts non achievable fractional order form of band limited transfer function into achievable rationalized model transfer function and it is,

$$C_{FR}(s) = C_{FRG} \prod_{i=1}^N \left(\frac{s + \omega'_i}{s + \omega_i} \right) \tag{11}$$

Where,

$$\frac{\omega'_{i+1}}{\omega'_i} = \frac{\omega_{i+1}}{\omega_i} = \alpha\eta \tag{12}$$

$$\frac{\omega_i}{\omega'_i} = \alpha \text{ and } \frac{\omega'_{i+1}}{\omega_i} = \eta \tag{13}$$

$$\alpha\eta = \left(\frac{\omega_h}{\omega_l} \right)^{1/N} \tag{14}$$

Where,

$$\begin{aligned} \alpha &= (\alpha\eta)^n \quad \text{and} \quad \eta = (\alpha\eta)^{1-n} \\ \omega'_i &= \omega_l \eta^{1/2} \quad \text{and} \quad \omega_N = \omega_h \eta^{-1/2} \end{aligned} \tag{15}$$

The elimination of phase undulation, it is to be selected value of N around 6. To achieve desired controller effort and elimination of steady states error to make series connection of band

limited integrator of order n_I and differentiator order of n_F . After that the complete transfer function of fractional order FGC is,

$$C_F(s) = C_0 \left(\frac{\omega_I}{s} + 1 \right)^{n_I} \left(\frac{1 + s/\omega_h}{1 + s/\omega_l} \right)^n \frac{1}{(1 + s/\omega_F)^{n_F}} \quad (16)$$

and the condition of,

$$\omega_l < \omega_l < \omega_{cg} > \omega_h > \omega_F, n_I = n_F = 1$$

Where the low pass filter and integrators are added for the purpose of reject the input noise disturbance and eliminate high frequency noise.

The steady state performance of FGC is achieved only proper selection of constant phase around ω_{cg} . But it is difficult to select ω_{cg} within the frequency band due controller effort limitations. So this will lead to development of SGC controller.

3.2. SGC Controller

Fig. 6 illustrates the block diagram of SGC [6] controller. The fractional order integrator open loop transfer function $\beta_s(s)$ is as follows,

$$\beta_S(s) = C_S(s) * G(s) = \left(\frac{\omega_{cg}}{s} \right)^n, n \in [1,2] \quad (17)$$

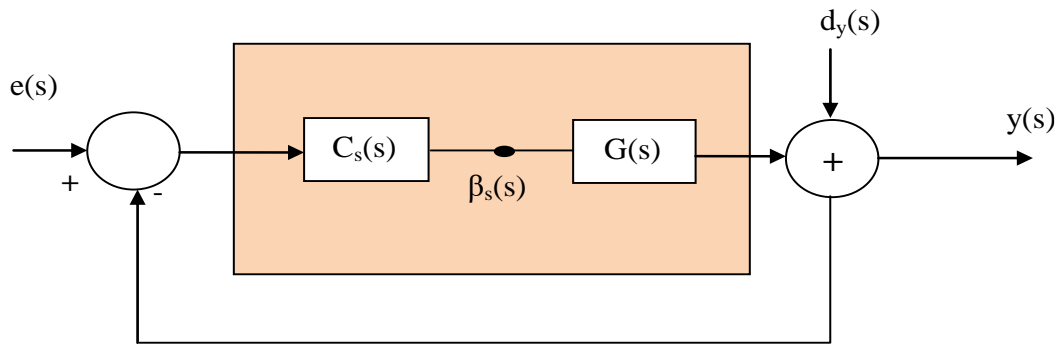


Fig. 6. Block diagram of SGC controller

The fractional order open loop transfer function of $\beta_s(s)$ is plotted in Black locus or Nichols plane [7] within range of frequency limit $[\omega_A, \omega_B]$ and it is shown in Fig. 7. The vertical straight line is formed in Nichols plane $\beta_s(s)$ is determined by the order of n around ω_{cg} . If any change in plant parameter will change the location of frequency template $\beta_s(s)$ vertically around ω_{cg} and this make assurance of quality of SGC [10] controller steady state response.

The overall fractional order open loop transfer function $\beta_s(s)$ is,

$$\beta_S(s) = K \left(\frac{\omega_I}{s} + 1 \right)^{n_I} \left(\frac{1 + s/\omega_h}{1 + s/\omega_l} \right)^n \frac{1}{(1 + s/\omega_F)^{n_F}} \quad (18)$$

Where $\omega_l < \omega_l < \omega_{cg} > \omega_h > \omega_F$. The chosen n_I and n_F values are depends on asymptotic behaviour of plant magnitude at the lower and higher value of frequencies.

The determined fractional order open loop transfer function of SGC [9] controller $C_s(s)$ from equation (17) is,

$$C_S(s) = \frac{\beta_S(s)}{G(s)} \quad (19)$$

Substituting the value of $\beta_S(s)$ from (10) in (11) becomes.

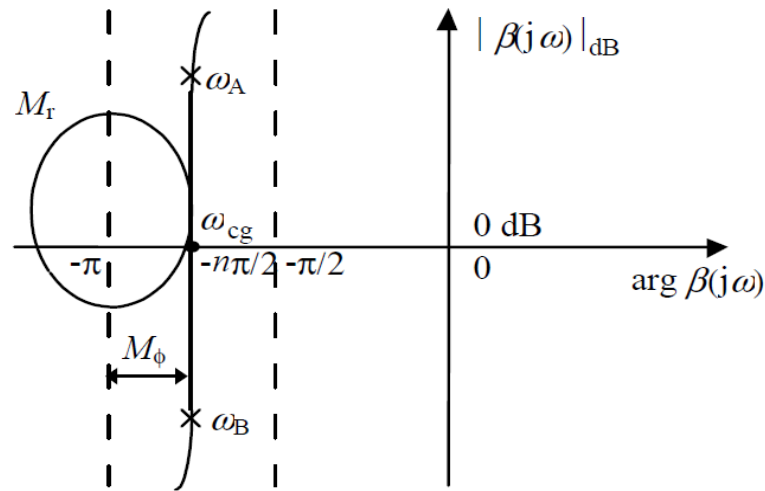


Fig. 7. Frequency template of $\beta_s(s)$

$$G_S(s) = \frac{K \left(\frac{\omega_l}{s} + 1\right)^{n_l} \left(\frac{1 + s/\omega_l}{1 + s/\omega_h}\right)^n \frac{1}{(1 + s/\omega_F)^{n_F}}}{G(s)} \quad (20)$$

3.3. Integer Order (IO) Relay Feedback PI Controller Design

Ziegler-Nichols method is widely used for PID, PI, and P controller tuning. In order to achieve instability in the system, this strategy first zeroes the integral and differential gains before increasing the proportional gain. Ultimate gain (K_u) is the value of K_p at the unstable point and Ultimate period (P_u) is the oscillation frequency. Astrom and Hagglund [46] have been recommended the generation of sustained oscillation by relay feedback method which is an alternative method to conventional continuous cycle technique to determine K_u and P_u of the system. By considering switch on and switch off points as 0.6 and 0.4 using relay feedback test method to compute ultimate period. The ultimate gain is finding out by making use of height (h) and amplitude (a) of oscillation.

$$K_u = \frac{4h}{\pi a} \quad (21)$$

The area $a=0.3$, $h=0.55$ and $P_u=2.6$ are obtained by using simulated response in Fig. 8 and substitute these values in equation (13), we get $K_u=2.335$. Finally the K_u and P_u values are used in closed loop transient Zeigler Nichols PID tuning rule [47] and find the PI [45] parameters of $K_c=1.43$ and $K_I=0.78$. The finding PI controller transfer function is,

$$G_c(s) = 1.42 + \frac{0.76}{s} \quad (22)$$

4. Design of CRONE Controller

The speed of the DCM speed can be controlled through CRONE MATLAB [51] and Simulink CSD toolbox, which is designed by CRONE research group.

4.1. FGC Controller

The transfer function of FGC controller is gained through speed control of DCM transfer function. For further analysis plant information of speed control DCM is applied in CRONE CSD toolbox and considered different perturbation of DCM. The perturbation gain change between the range is $0.09 < 1.01 < 1.1$. The CRONE CSD toolbox [51], [52] is applicable to solve for many problems like allowing, calculating, displaying and changing the parameters of fractional order and

rational form of CRONE controller and it has the Controller predefinition command allows setting the values of the parameters imposed by the user. The parameter predefinition of CRONE controllers are tabulated in Table 2.

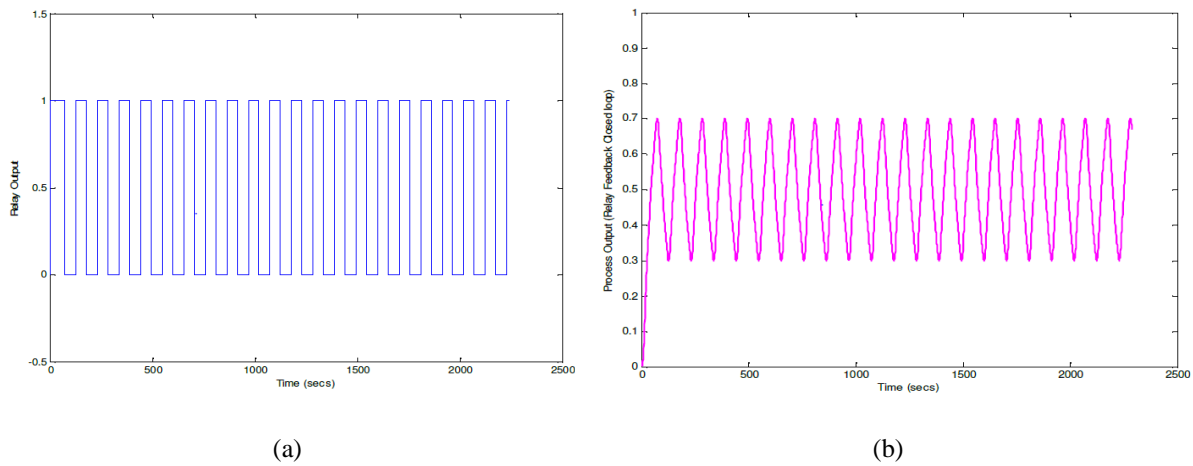


Fig. 8. (a) Relay output (b) Closed loop feedback output

Table 2. Parameter predefinition of CRONE fractional controller

Required nominal open loop gain cross over frequency - ω_{cg}	4	ω_A / ω_l ratio	10
Required nominal phase margin - P_m	54.432	ω_h / ω_B ratio	10
Integral order - n_i	1	$\omega_{AB} / \omega_{cg}$ ratio	1
Low-pass filter order - n_f	1	ω_{cg} / ω_i ratio	30
Fractional effect width - ω_A / ω_B ratio	2.1612	ω_f / ω_{cg} ratio	30
Approx. Cell no	5	-	-

The computed FGC values are given in Table 3.

Table 3. Fractional controller parameters of FGC

Gain C_0	17.3658
Integral order n_i	1
Frequency ω_i (rad/sec)	0.1
Fractional order n	-0.5569
Frequency ω_l (rad/sec)	0.20234
Frequency ω_h (rad/sec)	42.1679
Low pass filter order n_f	1
Filter Frequency ω_f (rad/sec)	90

Upon substituting values from Table 3 into equation (16), the fractional order FGC controller equation is presented below as,

$$G(s) = 17.3658 \left(\frac{0.20234}{s} + 1 \right)^1 \left(\frac{1 + (s/0.1)}{1 + s/42.1679} \right)^{-0.5569} \frac{1}{(1 + s/90)^1} \quad (23)$$

Similarly calculate the values of FGC rational controller given in the Table 4. By applying the rational values in the controller is further analysis as,

Fig. 9 depicts the responses of the FGC controller for applying various perturbations while using a simple unit step signal. The rational and fractional open loops Nichols charts of the SGC shown in Fig. 10.

$$C_R(s) = 91.0123X \frac{(s + 0.1)(s + 0.4778)(s + 1.237)(s + 3.8786)(s + 11.2334)(s + 32.59784)}{s(s + 0.2988)(s + 0.833)(s + 2.5345)(s + 6.675)(s + 19.612)(s + 90)} \quad (24)$$

Table 4. Rational controller parameters of FGC

Gain C	91.0123
Cell number	5
Recursive factor η	1.7655
Recursive factor β	1.767
Numerator corner frequencies ω_{ni} (rad/sec)	[0.1, 0.4778, 1.237, 3.8786, 11.2334, 32.59784]
Denominator corner frequencies ω_{ni} (rad/sec)	[0, 0.2988, 0.833, 2.5345, 6.675, 19.612, 90]

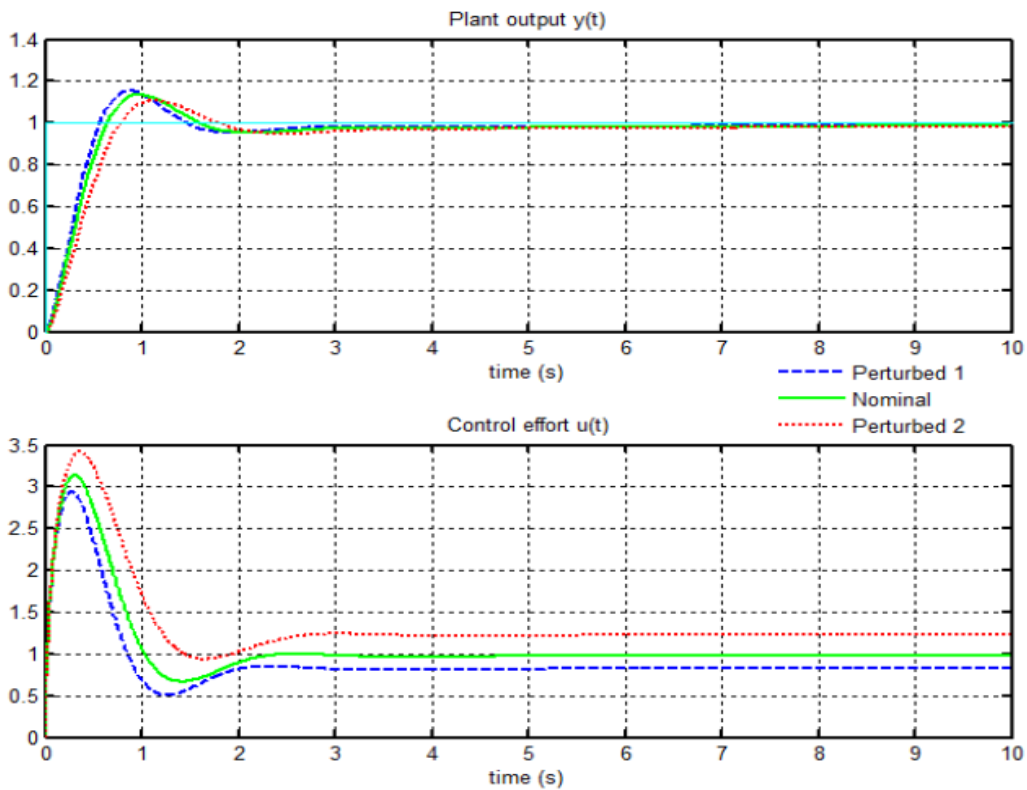


Fig. 9. FGC controller unit step closed loop response with their perturbations

4.2. SGC Controller

The technique for designing an SGC controller is similar to that of a FGC controller scheme. The simulation and fractional settings are validated and documented in [Table 5](#).

Table 5. SGC fractional controller parameter

Gain K	32.945
Low frequency order n_l	1
High frequency order n_h	3
Fractional order n	1.207
Frequency ω_l (rad/sec)	0.20234
Frequency ω_h (rad/sec)	42.1567
Fractional effect width ω_A / ω_B	2.0569
ω_A / ω_l ratio	10
ω_h / ω_B ratio	10

Substitute these tabulated values in equation (18) we get fractional order open loop transfer function is,

$$G(s) = 32.945 \left(\frac{0.20234}{s} + 1 \right)^1 \left(\frac{1 + (s/42.1567)}{1 + s/0.20234} \right)^{1.3307} \frac{1}{(1 + s/42.1567)^3} \quad (25)$$

The rationalized control parameters are determined and presented in Table 6.

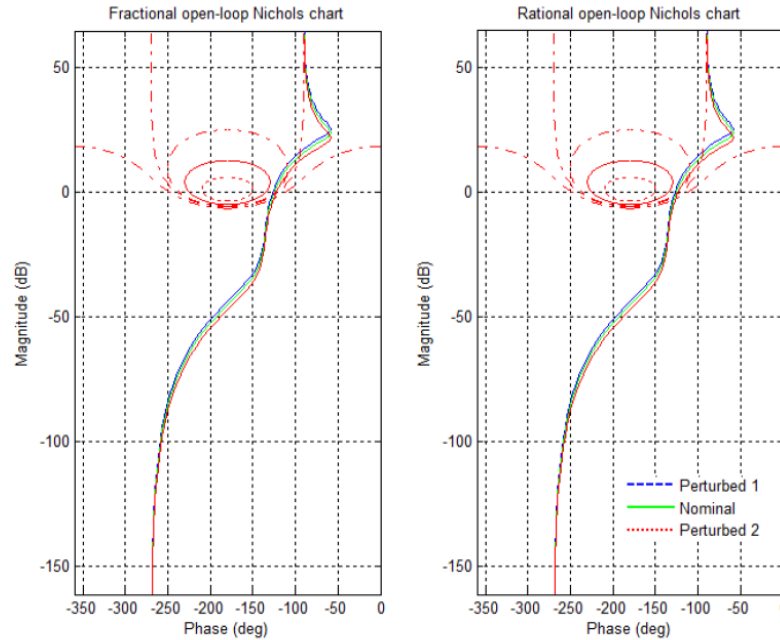


Fig. 10. FGC and rational open loop Nichols chart

Table 6. SGC fractional controller parameter

Gain C	26.678
Cell number	5
Recursive factor η	1.321
Recursive factor β	2.0234
Numerator corner frequencies ω_{ni} (rad/sec)	[0.436, 0.6938, 1.2615, 3.7834, 10.4289, 30.43896]
Denominator corner frequencies ω_{ni} (rad/sec)	[0, 0.6889, 0.9552, 2.3127, 7.32789, 21.5786, 43.21]

Depends on above parameters the SGC rationalized open loop transfer function is,

$$G(s) = 26.678X \frac{(s + 0.436)(s + 0.6938)(s + 1.2615)(s + 3.7834)(s + 10.4289)(s + 30.43896)}{s(s + 0.6889)(s + 0.9552)(s + 2.3217)(s + 7.32789)(s + 21.5786)(s + 43.21)} \quad (26)$$

Responses of SGC controller with applying simple unit step signal for the different perturbation is given in Fig. 11. The fractional and rational open loop Nichols charts of SGC given in Fig. 12.

5. Results and Discussion

The speed of DCM is controlled in this work by taking into account FGC, SGC, and Relay PI controllers. CSD tool box [51] is used to modify DCM speed during simulation performance, which is performed in MATLAB environment. When the DCM operates at varying speeds, the performance of the error and time indices is examined and noted. The set point tracking results were obtained at 40%, 50%, and 60% operating speeds, with distinct step changes applied to each operating speed. Simulation results for all three controllers are shown in terms of error and time domain indices. The response demonstrates the superiority of the CRONE controller system over the current conventional relay PI controller. Performance outcomes are recorded and summarized in Table 7 and Table 8.

The simulated comparison responses of the relay PI controller, applied to the plant transfer function of DCM, for the three distinct operating speeds, with ± 5 and $\pm 10\%$ step change, are displayed in Fig. 13.

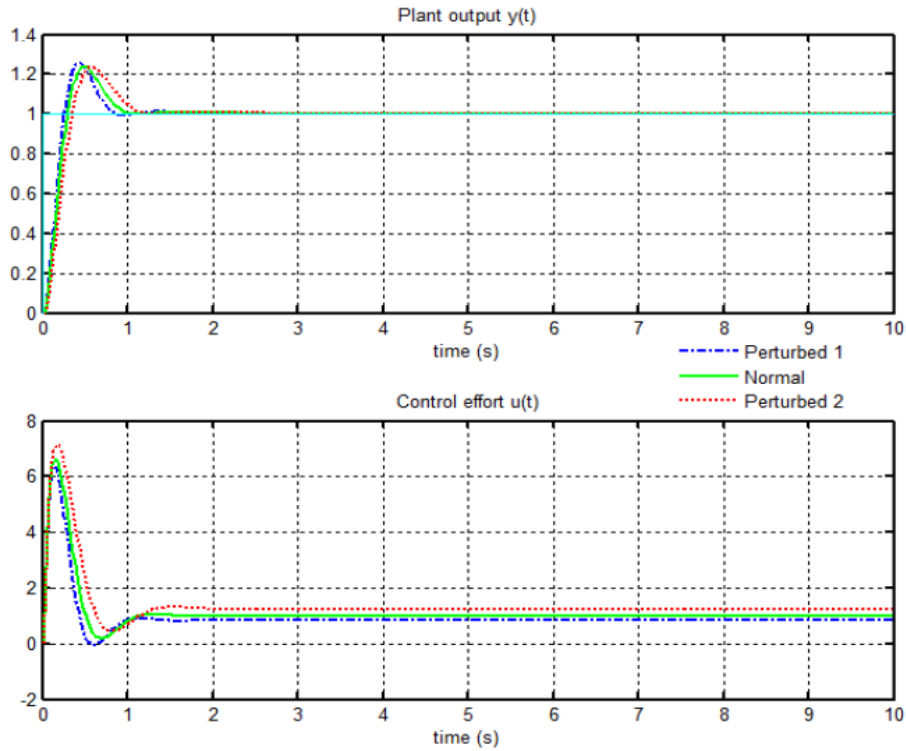


Fig. 11. SGC controller unit step closed loop response with their different perturbations

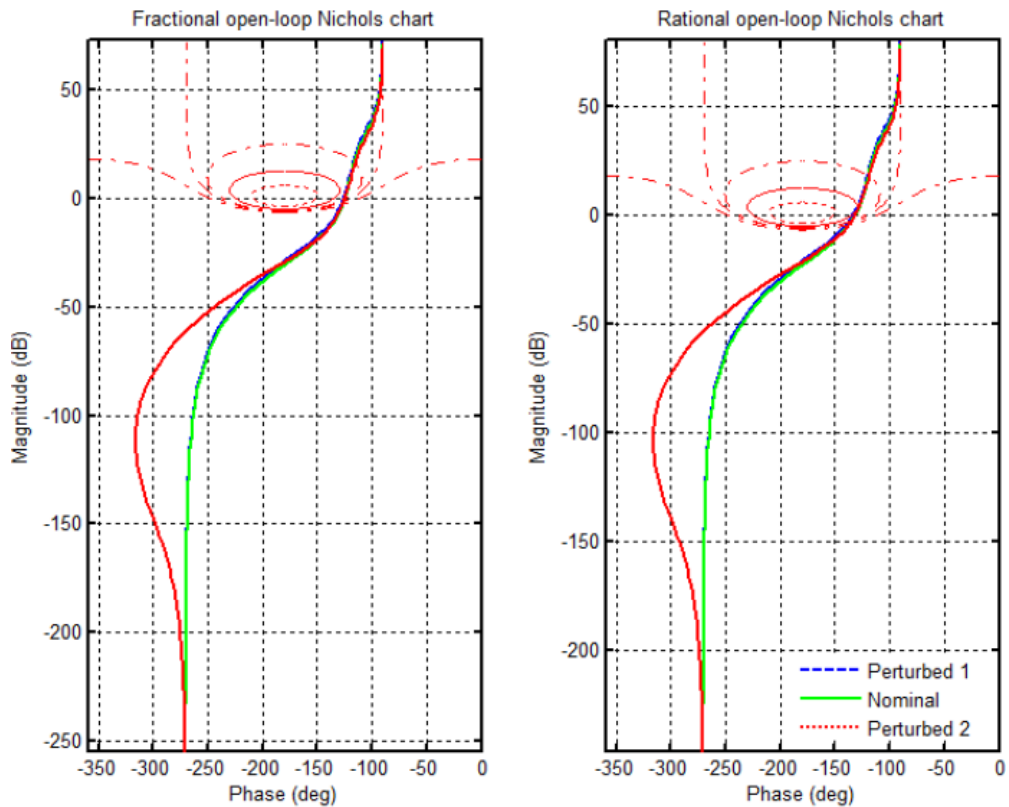
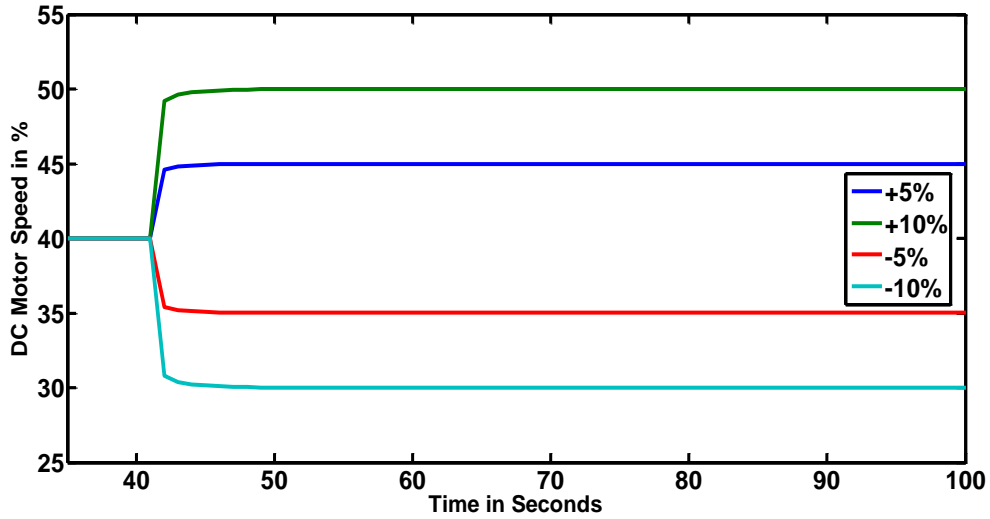
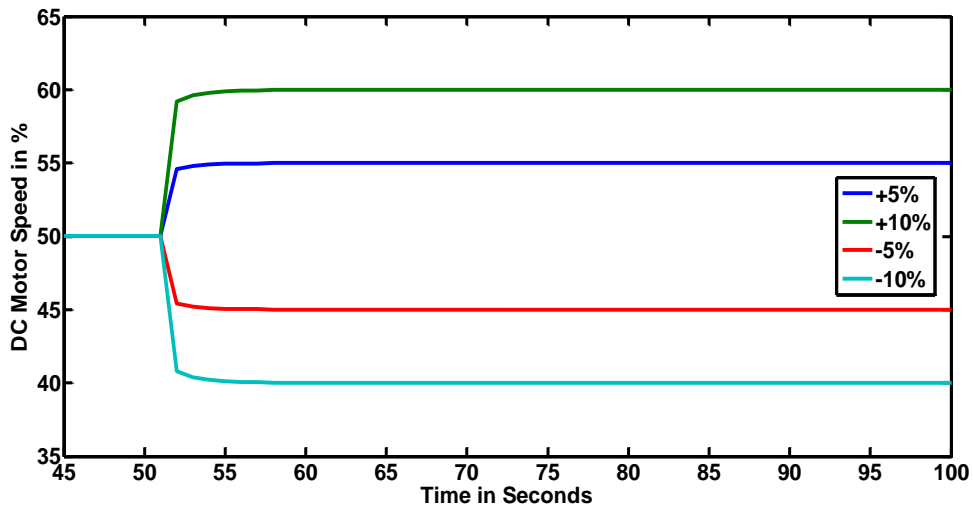


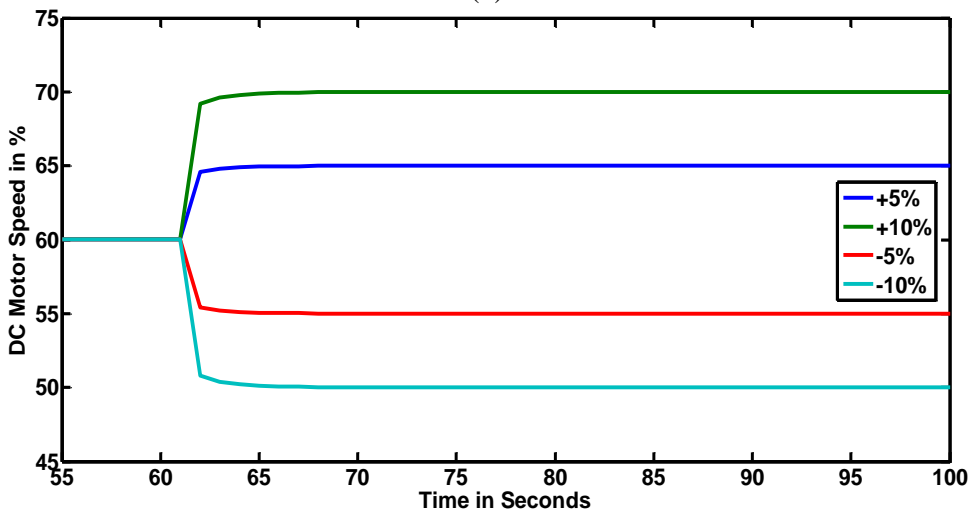
Fig. 12. SGC Fractional and rational open loop Nichols chart



(a)



(b)



(c)

Fig. 13. DCM Simulation: Set point tracking at (a) 40%, (b) 50%, (c) 60 % speed using R-PI controller

Fig. 14 displays the responses obtained for three distinct DCM running speeds, each with a different FGC controller perturbation and applied step changes of ± 5 and $\pm 10\%$ to the system.

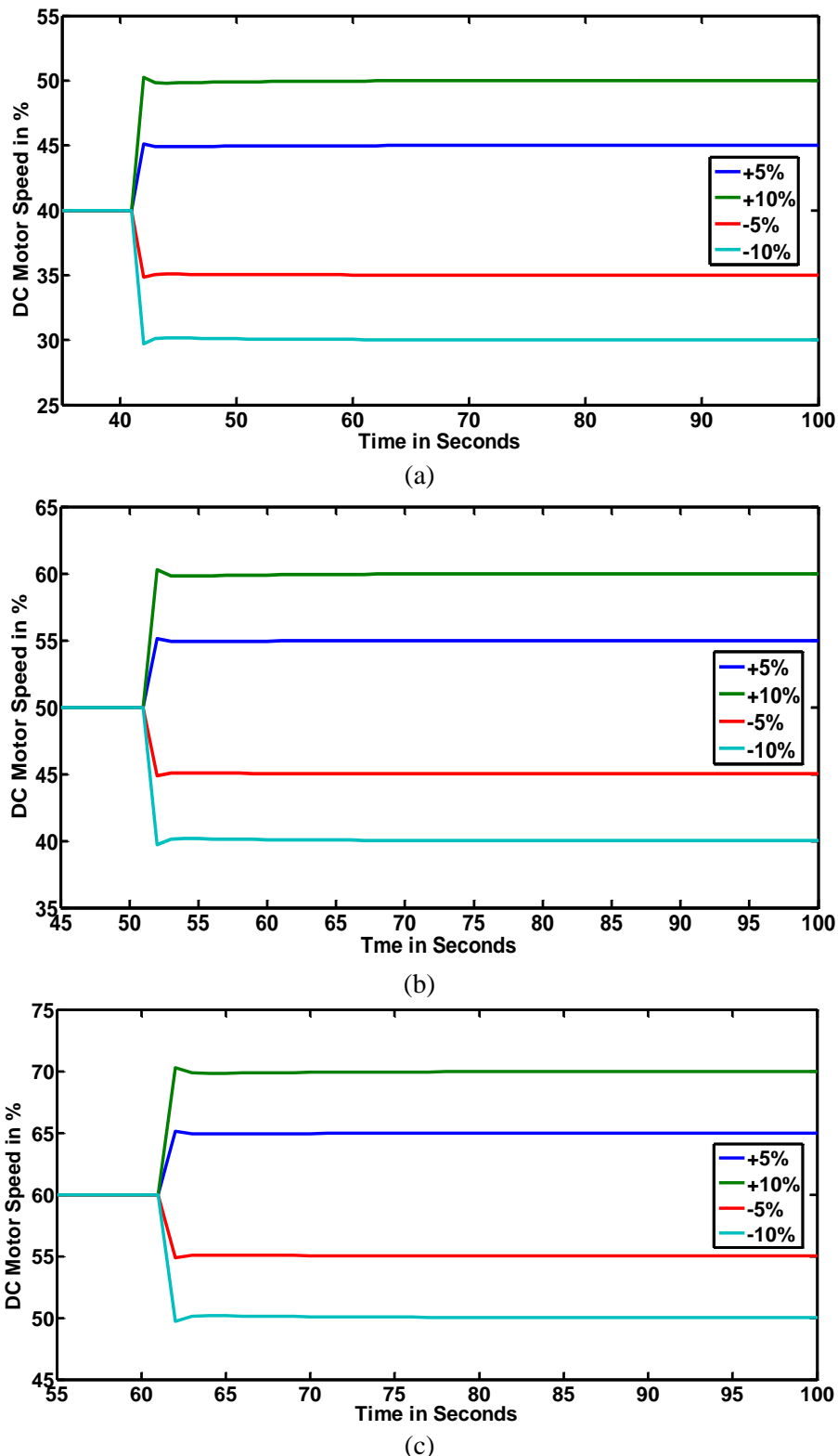
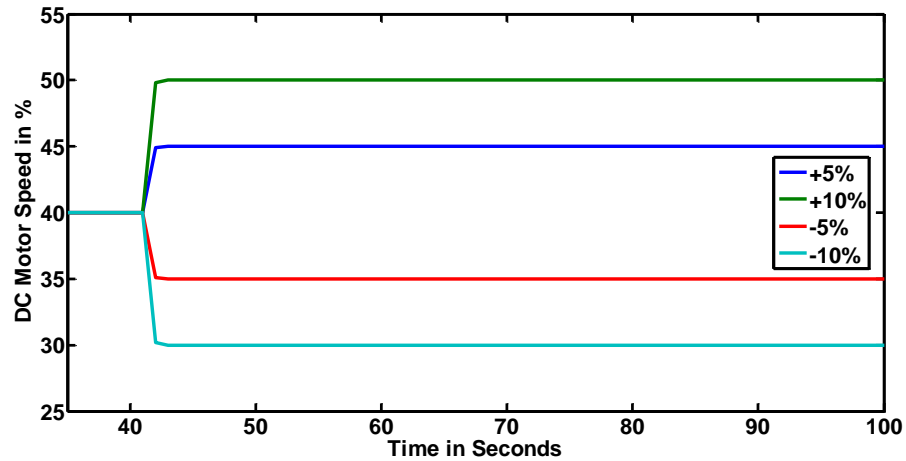
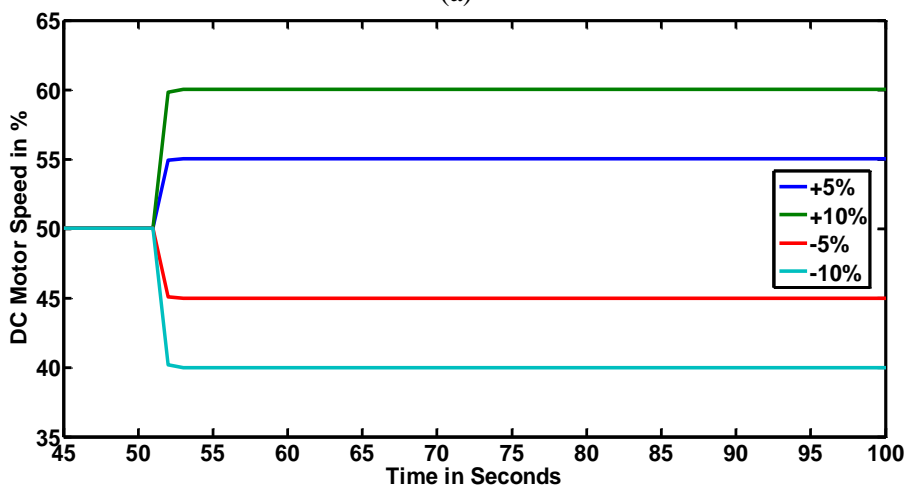


Fig. 14. DCM Simulation: Set point tracking at (a) 40%, (b) 50%, (c) 60 % speed using FGC controller

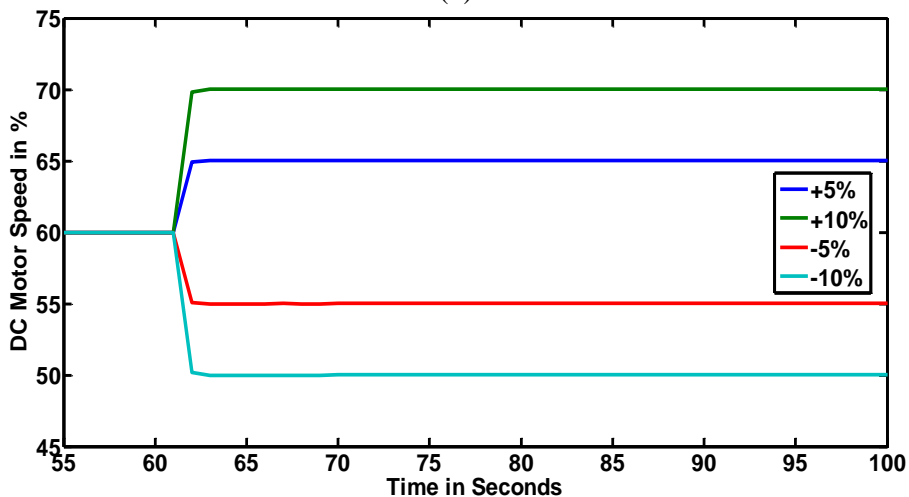
Fig. 15 illustrates the simulated time domain characteristics behavior of three distinct operating points with the SGC controller subjected to step changes of ± 5 and $\pm 10\%$. According to observations made of all three controllers, the relay PI controller's settling, rise time, ISE, and IAE are significantly lower than those of other CRONE controllers chosen for the mathematical model transfer function of the DCM's speed control. The SGC control performs the best out of the three.



(a)



(b)



(c)

Fig. 15. DCM Simulation: Set point tracking at (a) 40%, (b) 50%, (c) 60 % speed using SGC controller

Table 7 and Table 8 show the time domain characteristics of each of the three controllers for different operating points of the DCM's speed control. The robustness of these controllers is analyzed and reported in terms of error and time domain index performance through simulation in MATLAB using the CSD toolbox.

Table 7. DCM simulation: Set point tracking performance for controllers in terms of ISE and IAE at 40%, 50% and 60% speed

Operating Point	Step Change	R-PI		FGC		SGC	
		ISE	IAE	ISE	IAE	ISE	IAE
40%	+10%	292.6	25.69	260.6	22.47	243.6	13.8
	+5%	279.7	22.42	249.1	20.93	232.9	12.04
	-5%	279.7	22.42	249	20.58	232.9	12.04
	-10%	292.6	25.69	260.4	22.12	243.6	13.8
50%	+10%	447.6	30.23	398.5	27.58	372.6	16.05
	+5%	434.7	28.96	387	24.03	361.9	14.71
	-5%	434.7	27.96	386.9	24.87	361.9	14.71
	-10%	447.6	30.23	398.4	27.41	372.6	16.05
60%	+10%	636.9	35.77	567	31.65	530.3	18.73
	+5%	624	33.5	555.5	29.13	519.5	17.39
	-5%	624	33.5	555.5	29.05	519.5	17.39
	-10%	636.9	35.77	567	31.58	530.3	18.73

According to [Table 7](#), the Integral Squared Error (ISE) for the R-PI controller is 292.6, while the ISE value for the FGC controller is 260.6. This calculation is based on the simulation performance analysis for 40% of the running speed of the DCM with a step change of +10% applied to the controller. On the other hand, at a value of 243.6, the SGC controller offers the lowest value and greatest performance. Comparably, we found that the R-PI controller yielded an ISE value of 279.7, the FGC controller yielded an ISE value of 249.1, and finally, the SGC controller yielded an ISE value of 232.9, which was lower than that of the other selected controllers, at +5% step change given for the same operating point. Comparing the other two operating speed is done in the same way. The IAE value for the 50% operating speed with a -5% step change simulated results is 27.96 for the R-PI controller and 24.87 for the FGC controller. The third chosen SGC controller IAE value is only 14.71. Similarly, the controller is given a -10% step shift at the same working speed, and the IAE value is 30.23 for the R-PI controller, 27.41 for the FGC controller, and finally 16.05.

Therefore, it is confirmed that in every set point tracking scenario, the SGC controller performs better and ranks first due to its extremely low ISE and IAE values. All other findings are reported as well. The FGC performs significantly worse than the SGC controller and performs comparably better than the relay PI controller.

Table 8. DCM simulation: set point tracking performance for controllers in terms of t_s and t_r at 40%, 50% and 60% speed

Operating Point	Step Change	R-PI		FGC		SGC	
		t_s	t_r	t_s	t_r	t_s	t_r
40%	+10%	25	16	22	14	15	9
	+5%	22	14	20	12	12	8
	-5%	23	14	20	13	12	7
	-10%	25	17	23	14	14	8
50%	+10%	26	16	23	15	16	9
	+5%	23	14	20	13	12	7
	-5%	23	14	20	13	13	8
	-10%	27	17	23	14	15	9
60%	+10%	27	17	24	15	17	10
	+5%	24	14	21	13	12	9
	-5%	23	15	22	12	13	8
	-10%	26	16	23	15	16	9

Table 8 provides a comparative examination of the selected controller's settling time and rise time behaviour throughout three different DCM operation speeds. The R-PI controller is configured to operate at 60% of its maximum speed with a 10% step change, resulting in a settled time of 27 seconds, while the FGC is controlled at 24 seconds. In contrast, the SGC controller reaches steady state in just 17 seconds. Comparably, the R-PI controller yields a value of 16 in the case of rise time performance at the same operating speed of a -10% step change, whereas the accomplished FGC controller yields a value of 15. The SGC reached a rising time of 9.

Similarly, it is compared to other controller operating speeds. Therefore, it is clear from the foregoing data that, in terms of time indices performance, SGC controllers perform better than FGC controllers and relay PI controllers. By moving the relay PI controller to the last position, the FGC controller stays extremely near to the relay PI controller.

The error and time domain performance indices for the SGC, FGC, and R-PI controller methods are displayed graphically in Fig. 16 and Fig. 17, respectively, for running speeds of 40%, 50%, and 60% with different step changes.

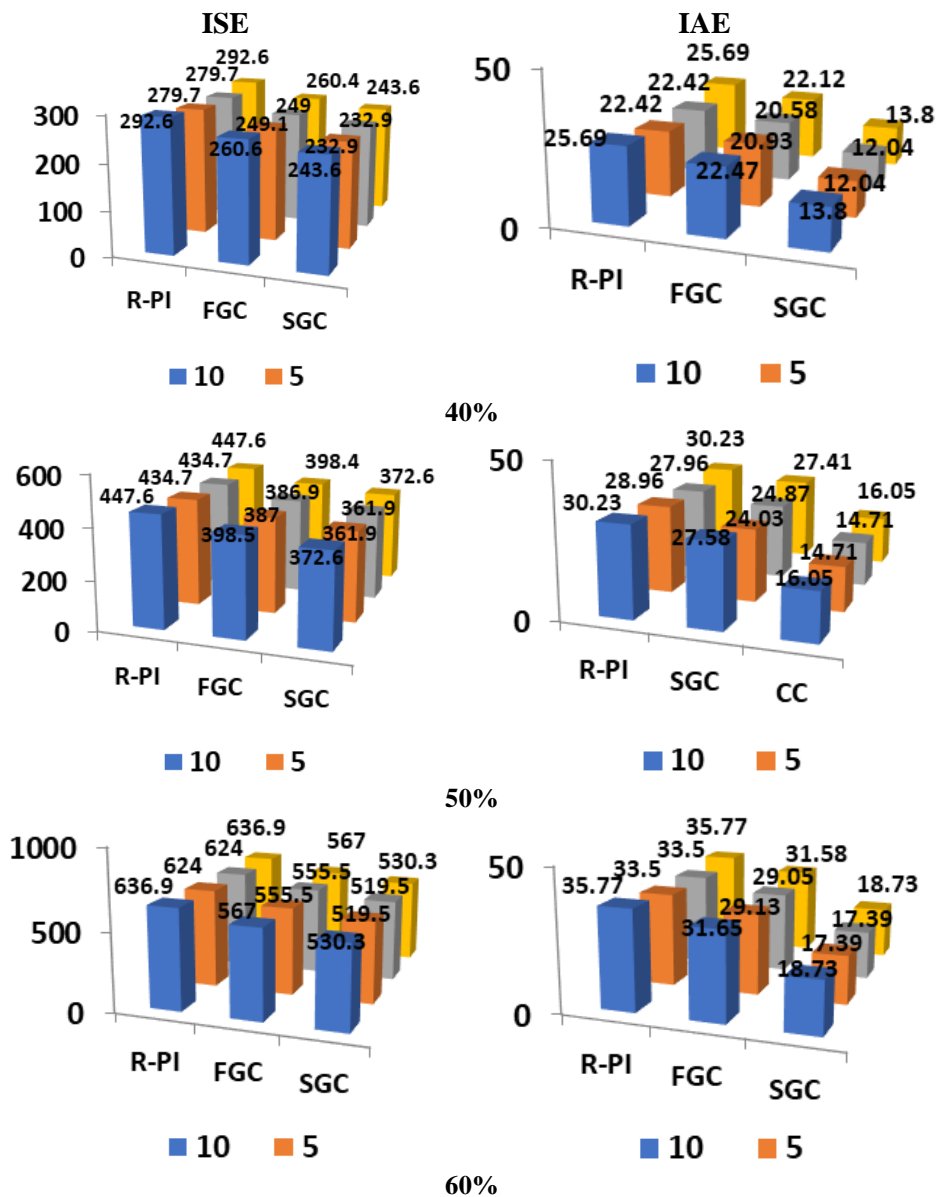


Fig. 16. Error indices (ISE and IAE) performances criteria

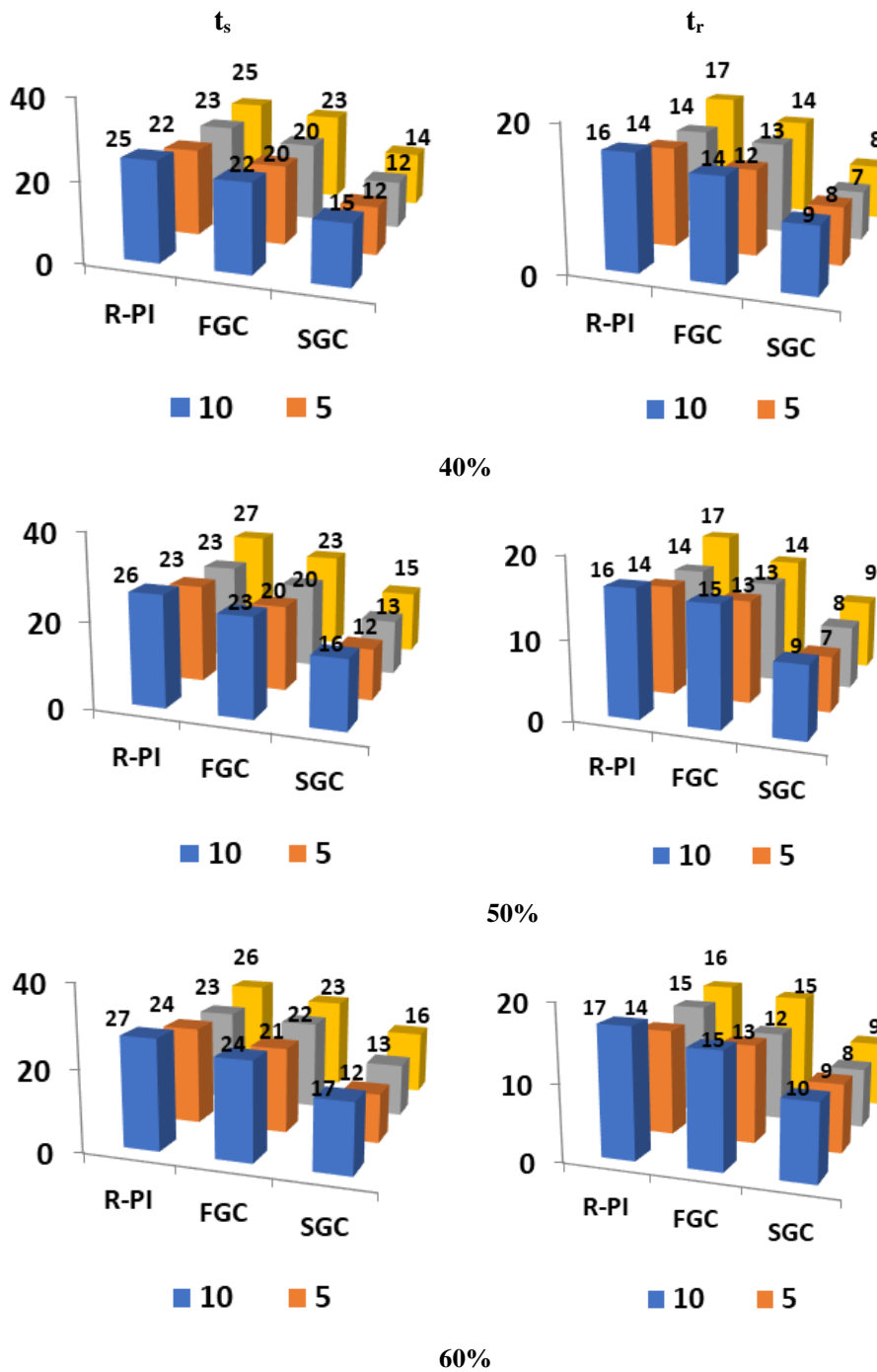


Fig. 17. Time Domain (t_s and t_r) performances criteria

6. Conclusion

In this research work, two generation of CRONE controllers and relay PI controllers are designed and implemented for speed control of DCM. The design strategy of CRONE controller is performed by CSD tool box in the MATLAB Simulink software. Simulations are used to get the reponses for three controllers with varied operating points in terms of settling time, rise time, ISE, and IAE. Furthermore, the performances are examined and provided. In summary of the solutions, it is found that SGC controller bestows improved performance than FGC controller and relay PI controller with respect to time indices performance.

Nomenclatures:

R_a - Armature (Electric) resistance (Ω)
 L_a - Armature (Electric) inductance (H)
 V_a - Armature voltage (V)
 J - Mass moment of inertia of motor (kg.m^2)
 B - Frictional coefficient of motor and load (Nm.s)
 i_a - Armature current, (amp)
 i_f - Field current, (amp)
 ω - Speed of the shaft (angular velocity), (rad/s)
 e_a - Input terminal voltage (source), (v)
 e_b - Back EMF, (v)
 T_q - Motor torque, (Nm)
 Θ - Motor Speed, (rpm)
 K_T - Torque factor constant, (Nm/amp)
 K_b - Motor constant, (v-s/rad)
 t_s - Settling time (Seconds)
 t_r - Rise time (Seconds)
 K_C - Controller proportional gain
 K_I - Controller Integral gain
 K_u - Ultimate gain
 P_u - Ultimate period
 $y_{\text{ref}}(s)$ - reference signal
 n - Fractional order transfer function order
 $C_S(s)$ - Second generation CRONE controller
 $C_{R-PI}(s)$ - Second generation CRONE controller
 $y(s)$ - plant output
 $\beta_S(s)$ - Second generation CRONE open loop fractional order transfer function
 $d_y(s)$ - Plant output disturbance
 $G(s)$ - Plant transfer function
 C_0 - Gain of the First generation CRONE controller
 $e(s)$ - Input reference signal
 $u(s)$ - Controller output
 $C_F(s)$ - First generation CRONE controller
 C_{FRG} - Gain of the First generation CRONE controller
 $C_{FR}(s)$ - Transfer function of Rational order First generation CRONE controller
 α and η - Recursive factor
 ω_{cg} - Open loop gain crossover frequency
 M_p - Phase margin
 M_r - Resonant peak
 n_I - Band limited integrator order
 n_F - Band limited low-pass filter order
 ω_I - Integrator frequency
 ω_F - Low-pass filter frequency
 $\omega_A, \omega_B, \omega_l, \omega_h$ - Band limited frequency
 ω_i and ω'_i - Distributed poles and zeros

Author Contribution: All authors contributed equally to the main contributor to this paper. All authors read and approved the final paper.

Funding: This research received no external funding.

Conflicts of Interest: The authors declare no conflict of interest

References

- [1] I. Birs, C. Muresan, I. Nascu and C. Ionescu, "A Survey of Recent Advances in Fractional Order Control for Time Delay Systems," *IEEE Access*, vol. 7, pp. 30951-30965, 2019, <https://doi.org/10.1109/ACCESS.2019.2902567>.
- [2] B. Yildirim, M. Gheisarnejad and M. H. Khooban, "A Robust Non-Integer Controller Design for Load Frequency Control in Modern Marine Power Grids," *IEEE Transactions on Emerging Topics in Computational Intelligence*, vol. 6, no. 4, pp. 852-866, 2022, <https://doi.org/10.1109/TETCI.2021.3114735>.
- [3] M. Gheisarnejad and M. H. Khooban, "An Intelligent Non-Integer PID Controller-Based Deep Reinforcement Learning: Implementation and Experimental Results," *IEEE Transactions on Industrial Electronics*, vol. 68, no. 4, pp. 3609-3618, 2021, <https://doi.org/10.1109/TIE.2020.2979561>.
- [4] M. H. Khooban, "An Optimal Non-Integer Model Predictive Virtual Inertia Control in Inverter-Based Modern AC Power Grids-Based V2G Technology," *IEEE Transactions on Energy Conversion*, vol. 36, no. 2, pp. 1336-1346, 2021, <https://doi.org/10.1109/TEC.2020.3030655>.
- [5] A. Oustaloup and M. Bansard, "First generation CRONE control," *Proceedings of IEEE Systems Man and Cybernetics Conference - SMC*, vol. 2, pp. 130-135, 1993, <https://doi.org/10.1109/ICSMC.1993.384861>.
- [6] A. Oustaloup, B. Mathieu and P. Lanusse, "Second generation CRONE control," *Proceedings of IEEE Systems Man and Cybernetics Conference - SMC*, vol. 2, pp. 136-142, 1993, <https://doi.org/10.1109/ICSMC.1993.384862>.
- [7] A. Oustaloup, X. Moreau and M. Nouillant, "From the second generation CRONE control to the CRONE suspension," *Proceedings of IEEE Systems Man and Cybernetics Conference - SMC*, vol. 2, pp. 143-148, 1993, <https://doi.org/10.1109/ICSMC.1993.384863>.
- [8] P. Melchior, A. Poty, B. Orsoni, A. Oustaloup, "Preshaping Command Inputs For 2nd Generation Crone Control: Application On An Instrumented Dc Motor Bench," *Proceedings of ASME, Design Engineering Technical Conferences and Computers and Information in Engineering Conference*, pp. 1-8, 2003, <https://doi.org/10.1115/DETC2003/VIB-48382>.
- [9] A. Oustaloup and P. Melchior, "The great principles of the CRONE control," *Proceedings of IEEE Systems Man and Cybernetics Conference - SMC*, vol. 2, pp. 118-129, 1993, <https://doi.org/10.1109/ICSMC.1993.384860>.
- [10] A. Oustaloup *et al.*, "An overview of the CRONE approach in system analysis, modelling and identification, observation and control," *IFAC Proceedings Volumes*, vol. 41, no. 2, pp. 14254-14265, 2008, <https://doi.org/10.3182/20080706-5-KR-1001.02416>.
- [11] S. E. Khadri, X. Moreau, A. Benine-Neto, M. Chevie, W. M. Goncalves, F. Guillemard, "Design of The CRONE Automatic Headlight Leveling System," *IFAC-PapersOnLine*, vol. 55, no. 27, pp. 208-213, 2022, <https://doi.org/10.1016/j.ifacol.2022.10.513>.
- [12] V. Velmurugan, and N. N. Praboo, "Crone Control Methodology for a Mechanical Active Suspension System," *Journal of Mechanics of Continua and Mathematical Sciences*, vol. 15, no. 10, pp. 1-19, 2020, <https://doi.org/10.26782/jmcms.2020.10.00001>.
- [13] B. Girirajan, D. Rathikarani, "Optimal CRONE controller using meta-heuristic optimization algorithm for shell and tube Heat Exchanger," *IOP Conference Series: Materials Science and Engineering*, vol. 1166, no. 1, p. 012058, 2021, <https://doi.org/10.1088/1757-899X/1166/1/012058>.
- [14] P. Lanusse, H. Benlaoukli, D. Nelson-Gruel, and A. Oustaloup, "Fractional-order control and interval analysis of SISO systems with time-delayed state," *IET Control Theory & Applications*, vol. 2, no. 1, pp. 16-23, 2008, <https://doi.org/10.1049/iet-cta:20060491>.
- [15] I. Petras, "Fractional-order feedback control of a DC motor," *Journal of Electrical Engineering*, vol. 60, no. 3, pp. 117-128, 2009, http://iris.elf.stuba.sk/jeeec/data/pdf/3_109-01.pdf.
- [16] D. Valerio, J. S. D. Costa, "Introduction to single-input, single-output fractional control," *IET Control Theory and Applications*, vol. 5, no. 8, pp. 1033-1057, 2010, <https://doi.org/10.1049/iet-cta.2010.0332>.

- [17] V. Kalyanaraman, P. K. Bhaba, "Design and Real Time Implementation of Fractional Order Proportional-Integral Controller (PI^λ) in A Liquid Level System," *Modern Applied Science*, vol. 5, no. 6, pp. 188-198, 2011, <https://doi.org/10.5539/mas.v5n6p188>.
- [18] C. A. Monje, B. M. Vinagre, V. Feliu, Y. Chen, "Tuning and auto-tuning of fractional order controllers for industry applications," *Control Engineering Practice*, vol. 16, no. 7, pp. 798–812, 2008, <https://doi.org/10.1016/j.conengprac.2007.08.006>.
- [19] I. Dimeas, I. Petras, C. Psychalinos, "New analog implementation technique for fractional order controller: A DC motor control," *International Journal of Electronics and Communications*, vol. 78, pp. 192-200, 2017, <https://doi.org/10.1016/j.aeue.2017.03.010>.
- [20] D. Izci, S. Ekincia, "Fractional order controller design via gazelle optimizer for efficient speed regulation of micromotors," *e-Prime - Advances in Electrical Engineering, Electronics and Energy*, vol. 6, p. 100295, 2023, <https://doi.org/10.1016/j.prime.2023.100295>.
- [21] H. F. Frayyeh, M. A. Mukhlif, A. M. Abbood, S. S. Keream, "Speed Control of Direct Current Motor using Mechanical Characteristics," *Journal of Southwest Jiaotong University*, vol. 54, no. 4, pp. 1-9, 2019, <https://doi.org/10.35741/issn.0258-2724.54.4.25>.
- [22] S. K. Suman and V. K. Giri, "Speed control of DC motor using optimization techniques based PID Controller," *2016 IEEE International Conference on Engineering and Technology (ICETECH)*, pp. 581-587, 2016, <https://doi.org/10.1109/ICETECH.2016.7569318>.
- [23] M. Owayjan, R. A. Z. Daou and X. Moreau, "The Effects of Nonlinearities on the Robustness of Various Controllers: Application on a DC Motor," *2018 IEEE International Multidisciplinary Conference on Engineering Technology (IMCET)*, pp. 1-6, 2018, <https://doi.org/10.1109/IMCET.2018.8603065>.
- [24] E. Guerrero, J. Linares, E. Guzman, H. Sira, G. Guerrero and A. Martinez, "DC Motor Speed Control through Parallel DC/DC Buck Converters," *IEEE Latin America Transactions*, vol. 15, no. 5, pp. 819-826, 2017, <https://doi.org/10.1109/TLA.2017.7910194>.
- [25] J. Yang, H. Wu, L. Hu and S. Li, "Robust Predictive Speed Regulation of Converter-Driven DC Motors via a Discrete-Time Reduced-Order GPIO," *IEEE Transactions on Industrial Electronics*, vol. 66, no. 10, pp. 7893-7903, 2019, <https://doi.org/10.1109/TIE.2018.2878119>.
- [26] I. Okoro and C. Enwerem, "Model-based Speed Control of a DC Motor Using a Combined Control Scheme," *2019 IEEE PES/IAS PowerAfrica*, pp. 1-6, 2019, <https://doi.org/10.1109/PowerAfrica.2019.8928856>.
- [27] Preeti, P. Mandal, K. Dutt, "Review on Speed Control of Dc Motor using PI & PI Fuzzy Logic Controller," *International Journal of Creative Research Thoughts*, vol. 9, no.11, pp. a800-a811, 2021, <https://ijcrt.org/papers/IJCRT2111101.pdf>.
- [28] J. Scott, J. McLeish and W. H. Round, "Speed Control With Low Armature Loss for Very Small Sensorless Brushed DC Motors," *IEEE Transactions on Industrial Electronics*, vol. 56, no. 4, pp. 1223-1229, 2009, <https://doi.org/10.1109/TIE.2008.2007046>.
- [29] N. Shaharudin, M. Z. Hasan, S. M. Noor, "Direct Current (DC) Motor Speed and Direction Controller," *Journal of Physics: Conference Series*, vol. 2129, no. 1, p. 012035, 2021, <https://doi.org/10.1088/1742-6596/2129/1/012035>.
- [30] N. Balakrishna, L. V. Kumar, S. Sandeep, D. D. Prasad, B. Srikanth, "Speed and Direction Control of DC Motor using Android Mobile Application," *EPRA International Journal of Research and Development*, vol. 7, no. 6, pp. 221-224 2022, <https://doi.org/10.36713/epra10539>.
- [31] S. Carriere, S. Caux, M. Fadel, "Optimised speed control in state space for PMSM direct drives," *IET Electric Power Applications*, vol. 4, no. 3, pp. 158–168, 2010, <https://doi.org/10.1049/iet-epa.2009.0080>.
- [32] A. Morand, X. Moreau, P. Melchior, M. Moze and F. Guillemard, "CRONE Cruise Control System," *IEEE Transactions on Vehicular Technology*, vol. 65, no. 1, pp. 15-28, 2016, <https://doi.org/10.1109/TVT.2015.2392074>.

-
- [33] A. G. Khiabani, R. Babazadeh, "Design of Robust Fractional-order Lead-Lag Controller for Uncertain Systems," *IET Control Theory & Applications*, vol. 10, no. 18, pp. 2447–2455, 2016, <https://doi.org/10.1049/iet-cta.2015.1293>.
- [34] R. S. Barbosa, J. A. T. Machado and A. M. Galhano, "Performance of fractional PID algorithms controlling nonlinear systems with saturation and backlash phenomena," *Journal of Vibration and Control*, vol. 13, no. 9-10, pp. 1407-1418, 2007, <https://doi.org/10.1177/1077546307077499>.
- [35] F. Meng, S. Liu, A. Pang and K. Liu, "Fractional Order PID Parameter Tuning for Solar Collector System Based on Frequency Domain Analysis," *IEEE Access*, vol. 8, pp. 148980-148988, 2020, <https://doi.org/10.1109/ACCESS.2020.3016063>.
- [36] P. Buenestado, J. Gibergans-Báguena, L. Acho, G. Pujol-Vázquez, "Predictive Speed Control of a DC Universal Motor Applied to Monitor Electric Vehicle Batteries," *Machines*, vol. 11, no. 7, p. 740, 2023, <https://doi.org/10.3390/machines11070740>.
- [37] J. U. Liceaga-Castro, I. I. Siller-Alcalá, J. Jaimes-Ponce, R. A. Alcántara-Ramírez, E. A. Zamudio, "Identification and Real Time Speed Control of a Series DC Motor," *Mathematical Problems in Engineering, Hindawi*, vol. 2017, 2017, <https://doi.org/10.1155/2017/7348263>.
- [38] S. Tufenkci, B. B. Alagoz, G. Kavuran, C. Yeroglu, N. Herencsar, S. Mahata, "A theoretical demonstration for reinforcement learning of PI control dynamics for optimal speed control of DC motors by using Twin Delay Deep Deterministic Policy Gradient Algorithm," *Expert Systems with Applications*, vol. 213, p. 119192, 2023, <https://doi.org/10.2139/ssrn.4123458>.
- [39] Z. S. Al-Sagar, M. S. Saleh, K. G. Mohammed, A. Z. Sameen, "Modelling and Simulation Speed Control of DC Motor using PSIM," *IOP Conference Series: Materials Science and Engineering*, vol. 745, no. 1, p. 012024, 2020, <https://doi.org/10.1088/1757-899X/745/1/012024>.
- [40] T. V. Moghaddam, N. Bigdeli, K. Afshar, "Tuning a Fractional Order PID Controller with Lead Compensator in Frequency Domain," *International Journal of Electrical and Electronics Engineering*, vol. 51, no. 3, pp. 139–144, 2011, https://www.idc-online.com/technical_references/pdfs/electrical_engineering/Tuning%20a%20Fractional.pdf.
- [41] M. Xiao, B. Tao, W. X. Zheng and G. Jiang, "Fractional-Order PID Controller Synthesis for Bifurcation of Fractional-Order Small-World Networks," *IEEE Transactions on Systems, Man, and Cybernetics: Systems*, vol. 51, no. 7, pp. 4334-4346, 2021, <https://doi.org/10.1109/TSMC.2019.2933570>.
- [42] S. J. Hammoodi, K. S. Flayyih, A. R. Hamad, "Design and implementation speed control system of DC Motor based on PID control and Matlab Simulink," *International Journal of Power Electronics and Drive System*, vol. 11, no. 1, pp. 127-134, 2020, <http://doi.org/10.11591/ijpeds.v11.i1.pp127-134>.
- [43] A. Varshney, D. Gupta, B. Dwivedi, "Speed Response of Brushless DC Motor using Fuzzy PID Controller under Varying Load Condition," *Journal of Electrical Systems and Information Technology, Science Direct*, vol. 4, no. 2, pp. 310-321, 2017, <https://doi.org/10.1016/j.jesit.2016.12.014>.
- [44] R. Goswami, D. Joshi, "Performance Review of Fuzzy Logic Based Controllers Employed in Brushless DC Motor," *Procedia Computer Science*, vol. 132, pp. 623-631, 2018, <https://doi.org/10.1016/j.procs.2018.05.061>.
- [45] C. Kannan, N. K. Mohanty, R. Selvarasu, "A new topology for cascaded H-bridge multilevel inverter with PI and Fuzzy control," *Energy Procedia*, vol. 117, pp. 917-926, 2017, <https://doi.org/10.1016/j.egypro.2017.05.211>.
- [46] K. J. Astrom, and T. Hagglund, "Automatic tuning of simple regulators with specifications on phase and amplitude margins," *Automatica*, vol. 20, no. 5, pp. 645–651, 1984, [https://doi.org/10.1016/0005-1098\(84\)90014-1](https://doi.org/10.1016/0005-1098(84)90014-1).
- [47] J. G. Zeigler, N. B. Nichols, "Optimum Setting for automatic controllers," *Journal of Fluids Engineering*, vol. 64, no. 8, pp.759-768, 1942, <https://doi.org/10.1115/1.4019264>.
- [48] S. W. Khubalkar, A. S. Junghare, M. V. Aware, A. S. Chopade, S. Das, "Demonstrative fractional order – PID controller based DC motor drive on digital platform," *ISA Transactions*, vol. 83, pp. 7983, 2018, <https://doi.org/10.1016/j.isatra.2017.08.019>.
-

- [49] K. Sabanci, "Artificial Intelligence Based Power Consumption Estimation of Two-Phase Brushless DC Motor According to FEA Parametric Simulation," *Measurement*, vol. 155, p. 107553, 2020, <https://doi.org/10.1016/j.measurement.2020.107553>.
- [50] B. N. Kommula, V. R. Kota, "Direct instantaneous torque control of Brushless DC motor using firefly Algorithm based fractional order PID controller," *Journal of King Saud University – Engineering Sciences*, vol. 32, no. 2, pp. 133-140, 2020, <https://doi.org/10.1016/j.jksues.2018.04.007>.
- [51] P. Lanusse, R. Malti and P. Melchior, "CRONE control system design toolbox for the control engineering community: tutorial and case study," *Philosophical Transactions of the Royal Society A: Mathematical, Physical and Engineering Sciences*, vol. 371, no. 1990, p. 20120149, 2013, <https://doi.org/10.1098/rsta.2012.0149>.
- [52] V. Tytiuk, O. Ilchenko, O. Chorny, I. Zachepa, S. Serhienko and A. Berdai, "SRM Identification with Fractional Order Transfer Functions," *2019 IEEE 2nd Ukraine Conference on Electrical and Computer Engineering (UKRCON)*, pp. 271-274, 2019, <https://doi.org/10.1109/UKRCON.2019.8879970>.